# Three-dimensional magnetic flux-closure domain patterns in MnAs thin films on GaAs(001)

R. Engel-Herbert and T. Hesjedal[a)]
*Magnetic Materials Laboratory, University of Waterloo, Waterloo, Ontario N2L 3G1, Canada*

D. M. Schaadt
*Paul-Drude-Institut für Festkörperelektronik, Hausvogteiplatz 5-7, D-10117 Berlin, Germany*

(Presented on 11 January 2007; received 17 October 2006; accepted 13 December 2006; published online 2 May 2007)

The magnetic microstructure of single-crystalline MnAs films on GaAs(001) has been investigated. Magnetic force microscopy (MFM) reveals a three-dimensional magnetization pattern that is in disagreement with the simple domain picture observed by surface-sensitive magnetic imaging. Here, we present a consistent micromagnetic picture of MnAs thin films in the ferromagnetic stripe phase, which appears in the course of the phase transition. A number of equilibrium magnetization patterns of the stripes are found that are, in fact, based on flux-closure domain patterns in the basal plane of MnAs. The simulation of a stripe array yields excellent agreement with the measured surface magnetization. The experimentally observed stray field contrast was confirmed by MFM contrast simulations based on these equilibrium magnetization patterns. © *2007 American Institute of Physics*. [DOI: 10.1063/1.2711421]

## I. INTRODUCTION

A prerequisite for spin-based electronics[1] are materials systems that combine ferromagnetic films with semiconductor substrates. The existence of ferromagnetic ordering above room temperature is hereby crucial. Manganese arsenide (MnAs) is one of the few ferromagnetic materials that can be grown epitaxially on GaAs and Si,[2] and that exhibits a Curie temperature above room temperature.[3] In MnAs/GaAs(001), spin-polarized carrier injection has been successfully demonstrated.[4] So far, the micromagnetic properties of MnAs/GaAs(001) have been imaged by stray field sensitive magnetic force microscopy[5] (MFM) and surface magnetization-sensitive x-ray magnetic circular dichroism with photoemission electron microscopy (XMCDPEEM).[6] The direct comparison of the magnetization distribution derived from both methods render, in principle, similar domain types.[7] In detail, however, large discrepancies become obvious that were discussed and partially resolved in Ref. 8. By combining the complementary experimental findings with three-dimensional micromagnetic simulations, we present a complete analysis of the magnetization distribution yielding rather surprising domain configurations, consistent with the experimental results.

## II. MATERIALS SYSTEM AND MICROMAGNETIC SIMULATIONS

MnAs can be grown epitaxially on GaAs(001) by molecular beam epitaxy, where the prismatic $(1\bar{1}00)$ plane of MnAs is the growth surface and the [0001] (*c* axis) and $[11\bar{2}0]$ (*a* axis) directions of MnAs are aligned along the $[1\bar{1}0]$ and [110] directions of GaAs, respectively.[9] For convenience, the growth direction is termed *b* axis (see Fig. 1). MnAs bulk crystals exhibit a uniaxial magnetocrystalline anisotropy, with the *c* axis being the hard axis of magnetization.[10] As a result of the shape anisotropy of the film that disfavors a magnetization normal to the film plane, an effective magnetic easy axis behavior along the in-plane *a*-axis direction is observed.[11]

In MnAs, ferromagnetic order vanishes at a temperature of ≈40 °C.[3] The transformation from ferromagnetic, hexagonal $\alpha$-MnAs to nonferromagnetic, orthorhombic $\beta$-MnAs proceeds continuously in thin films. The strain-stabilized $\alpha$-$\beta$-stripe structure (stripe axis along the *c* axis) is observed

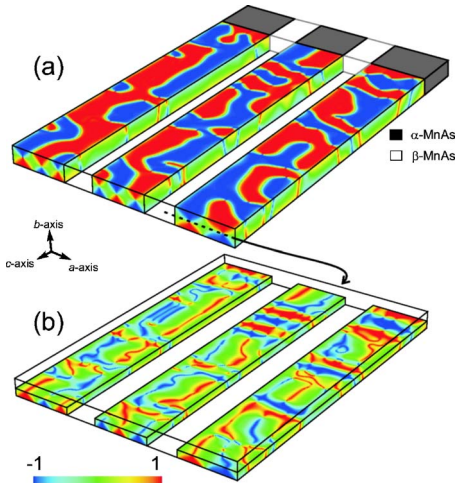


FIG. 1. (Color online) Simulated magnetization pattern of three ferromagnetic $\alpha$-MnAs stripes at zero field. (a) shows the surface magnetization ($M_a$ component, $b$=120 nm) and (b) the respective magnetization in the middle of the film ($b$=60 nm). In the upper right-hand side corner, the $\alpha$-$\beta$-stripe structure is sketched. The $\alpha$ stripes are 384 nm wide and separated by a 192-nm-wide $\beta$ stripe.

[a)]Author to whom correspondence should be addressed; electronic mail: t.hesjedal@ece.uwaterloo.ca

 

in a temperature window of 10–40 °C.[12] A sketch of the stripe pattern is shown in Fig. 1; the gray areas represent the ferromagnetic $\alpha$ phase that shows the magnetic contrast along the stripes.

Based on the observation of the surface magnetization by XMCDPEEM, but also supported by a simple interpretation of the stray field images by MFM, the ferromagnetic stripes reveal up to three domains in the *a*-axis direction.[5,8] In a recent investigation of the magnetization reversal, we found that the magnetization states in the basal plane are the dominating feature of the magnetization of the stripes.[7,8]

For the micromagnetic simulations, which were carried out using a finite difference code based on the Landau-Lifshitz-Gilbert (LLG) equation, we used the material constants as follows: exchange constant $A=1.0\times10^{-11}$ J/m, saturation magnetization $M_s=800$ kA/m, and magnetocrystalline anisotropy constant $K=-7.2\times10^5$ J/m$^3$.[8] A cuboidal cell size of 8 nm was used for all simulations.

## III. RESULTS AND DISCUSSION

The simulated magnetization distribution of a 120-nm-thick MnAs film in the stripe phase is shown in Fig. 1. Three 384 nm wide $\alpha$ stripes are separated by 192-nm-wide nonferromagnetic $\beta$ stripes. This geometry is experimentally observed at a temperature of 30 °C. For the simulation, a fully randomized initial magnetization was assumed. A closer look at the surface magnetization, which corresponds to the observed XMCDPEEM image,[14] reveals up to three oppositely magnetized areas on a single stripe along the *a*-axis direction [termed domain configuration type (I), (II), and (III); cf. Figs. 1 and 3]. From XMCDPEEM imaging alone, one could speculate the existence of head-to-head domains [types (II) and (III)], which are known to exist in thinner soft magnetic films due to the less severe energy penalty associated with the magnetic charges on their walls.[15] In MnAs films, however, type (II) and (III) domains are a unique feature of thicker films ($\gtrsim$100 nm), which is a result of the underlying domain patterns (see Fig. 2). Within the film [cf. cut at half of the film thickness in Fig. 1(b)], the magnetization is almost entirely oriented in the *b*-axis direction, i.e., pointing into or out of the film plane. Only in a few areas, which are characterized by a (local) type (I) domain character of the stripe, the magnetization observed on the film surface remains the same throughout the thickness of the stripe. As a consequence, it is clear that the stray field images obtained by MFM will contain a wealth of information about the magnetization below the surface.

Figure 3 shows the domain patterns in the basal plane of MnAs, extracted from the simulation presented in Fig. 1. We find a surprising variety of flux-closure patterns closely resembling the (metastable) magnetic states observed in thin film elements of moderate size (see Fig. 2).[13] The image pairs represent the *a* and *b* components of the magnetization, respectively. The terminology of the observed patterns is in accordance with the nomenclature in rectangular soft magnetic structures:[13] (a) C state, (b) S state, (c) Landau state, (d) single cross tielike, (e) double cross tielike, (f) diamond state, (g) combination of diamond state and cross tielike state, and (h) double diamond state.

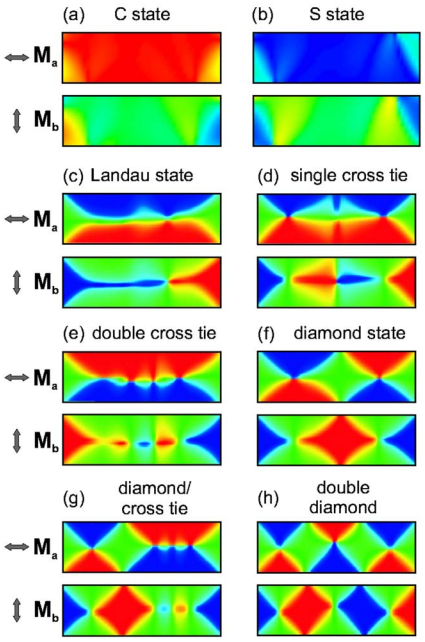


FIG. 2. (Color online) Magnetization patterns in the basal plane of MnAs (pairs of $M_a$ and $M_b$ images). The simulated domain patterns are extracted from the equilibrium magnetization of the stripe array shown in Fig. 1; $\alpha$ stripe of width 384 nm and film thickness of 120 nm. The nomenclature is referring to similar patterns observed in rectangular soft magnetic thin film structures (see, e.g., Ref. 13).

For observing a type (I) domain on the surface, the basal plane state can either be a C state, S state, Landau state, a single cross tielike pattern, or a double cross tielike pattern. Type (II) domains are the effect of a diamond state or a combination of a diamond state and a cross tielike state, whereas type (III) domains are connected to the double diamond state.

To simulate the surface magnetization and stray field contrast of the standard domain types (I–III), we filled the

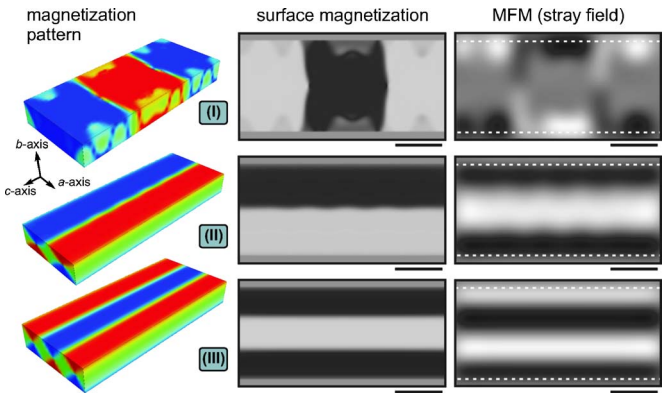


FIG. 3. (Color online) Left column: magnetization distribution for the relaxed, extended standard domain types (I), (II), and (III); $\alpha$ stripe of width 384 nm, film thickness of 120 nm, and stripe length of 880 nm. Middle column: respective surface magnetization ($M_a$ component) corresponding to the XMCDPEEM contrast. Right column: simulated MFM response for the three domain types. The black markers correspond to 200 nm.

stripe along the *c* axis (stripe length of 880 nm) with the the numerically derived cross sections associated with the respective domain type (cf. Fig. 1). The magnetization patterns created this way were allowed to relax, yielding the results shown in Fig. 3 in the left column. Whereas the type (II) and (III) domains, which originate from one and two extended diamond-shaped cross-sectional domains, respectively, relaxed readily, extended type (I) domains behave differently. Due to the large demagnetization energy, extended type (I) domains based on the C and S states are not stable upon relaxation for the given combination of geometry and saturation magnetization. Nevertheless, extended type (I) domains can become stable in narrower ferromagnetic stripes or in coupled stripe arrays. Thus, we assumed a different initial magnetization which is found in experimental MFM images. This alternating sequence of type (I) domains is stable upon relaxation. All three domain patterns are in agreement with the observed XMCDPEEM contrast representing the surface magnetization, shown in the middle column in Fig. 3.

For obtaining the MFM contrast, we treated the entire tip-sample system in the micromagnetic simulation scan point by scan point and calculated the force gradient of the magnetostatic interaction at each scan position. For simplicity, we assumed mutual nondisturbance of tip and sample and a finite micromagnetic model for the tip. The tip-sample volume discretization was 6 nm in all three dimensions. Reference[16] contains details of the simulation procedure. The right column in Fig. 3 (top) shows the MFM response (force gradient) for three oppositely magnetized, neighboring type (I) domains. To capture the MFM contrast outside the ferromagnetic stripes, a laterally increased sample volume was considered. The edge of the stripe is indicated by a dashed, bright line. The MFM contrast is characterized by dark and bright areas at the edges of the stripe. In between, 180° Bloch walls separate the oppositely magnetized areas. They show both bright and dark contrast as the magnetization rotates through both the $-b$ and $+b$ directions. The MFM contrast for type (II) is symmetric with respect to the stripe axis (along the *c* axis). A bright area in the middle is due to the out-of-plane moments of the underlying diamond domain structure. Type (III) domains result in a MFM contrast that is governed by the out-of-plane moments of the two diamond-shaped domains in the basal plane. Since the magnetization of the two diamond states is opposite, the MFM contrast shows bright and dark areas, respectively.

## IV. CONCLUSIONS

In summary, we present a consistent micromagnetic picture of MnAs thin films in the stripe phase, i.e., on GaAs(001). The magnetization patterns that lead to the domain types (I–III) were identified by micromagnetic simulations. The equilibrium magnetization pattern of coupled stripes reveal a surprising number of flux-closure domain patterns in the basal plane of MnAs. Type (I) domains were identified to be based on a C, S, Landau, or single or double cross tie wall-like state; type (II) domains on a diamond state or a combined diamond and single cross tie wall-like state; and type (III) domains on a double-diamond state. Through MFM contrast simulations, the three-dimensional magnetization patterns can be confirmed experimentally.

## ACKNOWLEDGMENTS

The authors want to thank the BMBF of Germany for partial financial support and K. H. Ploog for his continuous and generous support. One of the authors (R.E.H.) acknowledges partial financial support by NSERC of Canada.

[1] G. A. Prinz, Science **250**, 1092 (1990).
[2] M. Tanaka, J. P. Harbison, M. C. Park, Y. S. Park, T. Shin, and G. M. Rothberg, Appl. Phys. Lett. **65**, 1964 (1994).
[3] B. T. M. Willis and H. P. Rooksby, Proc. Phys. Soc. London, Sect. B **67**, 290 (1954).
[4] M. Ramsteiner *et al.*, Phys. Rev. B **66**, 081304 (2002).
[5] R. Engel-Herbert, J. Mohanty, A. Ney, T. Hesjedal, L. Däweritz, and K. H. Ploog, Appl. Phys. Lett. **84**, 1132 (2004).
[6] L. Däweritz *et al.*, J. Vac. Sci. Technol. B **23**, 1759 (2005).
[7] R. Engel-Herbert, T. Hesjedal, J. Mohanty, D. M. Schaadt, and K. H. Ploog, J. Appl. Phys. **98**, 063909 (2005).
[8] R. Engel-Herbert, T. Hesjedal, J. Mohanty, D. M. Schaadt, and K. H. Ploog, Phys. Rev. B **73**, 104441 (2006).
[9] F. Schippan, G. Behme, L. Däweritz, K. H. Ploog, B. Dennis, K.-U. Neumann, and K. R. A. Ziebeck, J. Appl. Phys. **88**, 2766 (2000).
[10] R. W. De Blois and D. S. Rodbell, Phys. Rev. **130**, 1347 (1963).
[11] J. Lindner *et al.*, J. Magn. Magn. Mater. **277**, 159 (2004).
[12] V. M. Kaganer, B. Jenichen, F. Schippan, W. Braun, L. Däweritz, and K. H. Ploog, Phys. Rev. Lett. **85**, 341 (2000).
[13] W. Rave and A. Hubert, IEEE Trans. Magn. **36**, 3886 (2000).
[14] R. Engel-Herbert *et al.*, Appl. Phys. A: Mater. Sci. Process. **A84**, 231 (2006).
[15] A. Hubert and R. Schäfer, *Magnetic Domains* (Springer, Berlin, 1998).
[16] R. Engel-Herbert, D. M. Schaadt, and T. Hesjedal, J. Appl. Phys. **99**, 113905 (2006).